American College of Neuropsychopharmacology

ARTICLE

mGluR5 in hippocampal CA1 pyramidal neurons mediates stress-induced anxiety-like behavior

Xin Li[1,2], Zhuo-Jun Du[1,2], Jun-Nan Xu[1], Zhi-Man Liang[1], Song Lin[1], Hao Chen[1], Shu-Ji Li[1], Xiao-Wen Li[1], Jian-Ming Yang[1] and Tian-Ming Gao[1]✉

Pharmacological manipulation of mGluR5 has showed that mGluR5 is implicated in the pathophysiology of anxiety and mGluR5 has been proposed as a potential drug target for anxiety disorders. Nevertheless, the mechanism underlying the mGluR5 involvement in stress-induced anxiety-like behavior remains largely unknown. Here, we found that chronic restraint stress induced anxiety-like behavior and decreased the expression of mGluR5 in hippocampal CA1. Specific knockdown of mGluR5 in hippocampal CA1 pyramidal neurons produced anxiety-like behavior. Furthermore, both chronic restraint stress and mGluR5 knockdown impaired inhibitory synaptic inputs in hippocampal CA1 pyramidal neurons. Notably, positive allosteric modulator of mGluR5 rescued stress-induced anxiety-like behavior and restored the inhibitory synaptic inputs. These findings point to an essential role for mGluR5 in hippocampal CA1 pyramidal neurons in mediating stress-induced anxiety-like behavior.

Neuropsychopharmacology (2023) 48:1164–1174; https://doi.org/10.1038/s41386-023-01548-w

INTRODUCTION

Anxiety disorders, defined as excess worry, hyperarousal and fear, are among the most prevalent psychiatric disorders in the worldwide [1, 2]. The prevalence of anxiety disorders is high across the globe and the lifetime prevalence estimates is 28.8% [3]. However, the mechanisms underlying the pathophysiology of the anxiety remains unclear and current treatments for anxiety disorders are not satisfying [4, 5]. Chronic stress is a key risk factor for anxiety disorders in human and can induce anxiety-like behavior in rodents, which is a widely used animal model for understanding the mechanisms of anxiety disorders [6, 7].

Glutamate is the prominent excitatory neurotransmitter in the brain [8]. Metabotropic glutamate receptors (mGluRs), which are a member of G-protein coupled receptors, could sense glutamate in the synaptic cleft [9–11]. Previous studies have showed that mGluR5 might be a potential drug target for anxiety disorders [12–15]. However, whether and how mGluR5 participates in chronic stress-induced anxiety-like behavior remains little known.

The hippocampus is traditionally thought to be important in modulating learning and memory [16–18]. Nevertheless, the hippocampus is also recognized as an important brain region to transmit contextual information to the limbic structures [19–22]. It has been reported that hippocampal CA1 is enriched in anxiety cells and responsible for anxiety-like behavior [23].

In this study, we investigated whether mGluR5 in the hippocampus participates in anxiety disorders through chronic restraint stress model. We found that chronic restraint stress induced anxiety-like behavior and reduced the inhibitory synaptic inputs in the hippocampal CA1 pyramidal neurons. Moreover, chronic restraint stress decreased the expression of mGluR5 in hippocampal CA1. Knockdown of mGluR5 in hippocampal CA1 pyramidal neurons produced anxiety-like behavior and impaired the inhibitory synaptic inputs. Positive allosteric modulator of mGluR5 rescued stress-induced anxiety-like behavior and restored the inhibitory synaptic inputs in hippocampal CA1 pyramidal neurons. Our findings demonstrate an essential role for mGluR5 in regulating stress-induced anxiety-like behavior.

MATERIALS AND METHODS

Mice

The mice (on C57BL/6 background) were housed in standard laboratory cages (3–5 per cage) under a 12 h light/dark cycle (lights on at 8:00 A.M.) in a temperature-controlled room (21–25 °C). The mice had free access to water and food. Behavioral testing was performed during the light cycle between 0:00 P.M. and 5:00 P.M. Only male mice were used in all experiments. All procedures were conducted in accordance with the Chinese Council on Animal Care Guidelines and were approved by the Southern Medical University Animal Ethics Committee. Efforts were made to minimize animal suffering. The mGluR5 loxp mice were obtained from the Jackson Lab. C57BL/6 mice (aged 8 weeks) were purchased from the Guangdong Medical Laboratory Animal Center (Guangzhou, China).

Restraint stress

The mice were individually placed head-first into well-ventilated 50 ml polypropylene conical tubes and tied with a cap of the 50 ml tube (2 h per day, 5 days). After each session of restraint stress, the mice were returned to their home cage, in which they had free access to food and water.

[1]State Key Laboratory of Organ Failure Research, Institute of Brain Diseases, Nanfang Hospital, Southern Medical University; Key Laboratory of Mental Health of the Ministry of Education, Guangdong-Hong Kong-Macao Greater Bay Area Center for Brain Science and Brain-Inspired Intelligence, Guangdong Province Key Laboratory of Psychiatric Disorders, Department of Neurobiology, School of Basic Medical Sciences, Southern Medical University, Guangzhou, China. [2]These authors contributed equally: Xin Li, Zhuo-Jun Du. ✉email: tgao@smu.edu.cn

Received: 10 October 2022 Revised: 18 January 2023 Accepted: 6 February 2023
Published online: 16 February 2023

Drugs and chemicals
Bicuculin, DNQX, AP-5 were purchased from Tocris Bioscience. CDPPB were purchased from Topscience (Shanghai, China). CDPPB was dissolved in DMSO to a concentration of 10 mg/ml, and mixed with PBS containing 10% Tween-80 in a 1:9 ratio for intraperitoneal injection. When DMSO (Sigma) was used to prepare solutions, its final concentration was 0.05% or less.

Antibodies
The primary antibodies were as follows: rabbit anti-mGluR5 (1:50, Abcam, ab76316), mouse anti-β-actin (1:100, Proteintech).

Slice preparation
The mice were anesthetized with ethyl ether and subsequently decapitated. The brains were quickly removed and placed in ice-cold oxygenated modified ACSF containing 220 mM sucrose, 2.5 mM KCl, 1.3 mM $CaCl_2$, 2.5 mM $MgSO_4$, 1 mM NaH_2PO_4, 26 mM $NaHCO_3$, and 10 mM glucose. 300 μm slices were prepared using a VT-1200S vibratome (Leica, Germany). Then the slices were transferred to a storage chamber containing normal ACSF (120 mM NaCl, 2.5 mM KCl, 1.2 mM NaH_2PO_4, 2.0 mM $CaCl_2$, 2.0 mM $MgSO_4$, 26 mM $NaHCO_3$, and 10 mM glucose) for a 30 min recovery period at 34 °C and subsequently at room temperature (25 ± 1 °C) for an additional 2-6 h. All solutions were saturated with 95% O_2/ 5% CO_2 (vol/vol).

Electrophysiological recordings
The slices were placed in a recording chamber perfused with ACSF (2 ml/min) at 32–34 °C. Whole-cell patch-clamp recordings of hippocampal neurons were obtained under 40X water-immersion lens (BX51WI, Olympus). Pipettes were pulled using a micropipette puller (P-97, Sutter instrument) with a resistance of 3–6 MΩ. Recordings were obtained using a MultiClamp 700 B amplifier and 1440 A digitizer (Molecular Device). For sEPSC and mEPSC recordings, glass pipettes were filled with a solution containing 125 mM Cs-methanesulfonate, 5 mM CsCl, 10 mM Hepes, 0.2 mM EGTA, 1 mM MgCl2, 4 mM Mg-ATP, 0.3 mM Na-GTP, 10 mM phosphocreatine and 5 mM QX314 (pH 7.40, 285 mOsm). For sIPSC and mIPSC recordings, the holding potentials were 0 mV, glass pipettes were filled with a solution containing 110 mM Cs_2SO_4, 0.5 mM $CaCl_2$, 2 mM $MgCl_2$, 5 mM EGTA, 5 mM HEPES, 5 mM TEA, 5 mM ATP-Mg, pH 7.35, 285 mOsm.

Western blot
The tissue was harvested and lysed in ice-cold RIPA lysis buffer (ThermoFisher) containing 1 mmol/L PMSF. For western blot, the proteins were detected by automatic protein detection instrument (ProteinSimple) and analysed by Compass software (ProteinSimple). The results were normalized to internal controls.

Quantitative real-time RT-PCR
The tissue was harvested and immediately extracted for total RNA and total RNA was reverse transcribed and amplified. The reverse transcription was conducted by using PrimeScript RT reagent kit (Takara, RR037A) and RT-qPCR analyses were performed using SYBR Premix Ex Taq (Takara, RR420A). The following sequences of primers were used for real-time RT-PCR. *GAPDH* forward: 5′-CAA TGT GTC CGT CGT GGA TCT-3′; *GAPDH* reverse: 5′-GTC CTC AGT GTA GCC CAA GAT G-3′. *mGluR5* forward: 5′-TTT GGA GTG CTG ACC AGG AG-3′; *mGluR5* reverse: 5′-AGG TTG ACT TTT TGG TCC CAG A-3′.

Stereotaxic microinjection
The mice were anesthetized with 1% pentobarbital sodium and placed in a stereotaxic frame. All coordinates are reported relative to the bregma in mm. The mortality rate was 0. The post-operative recovery time was generally ≥4 weeks. The scalp was incised and a hole drilled into the skull above the hippocampus CA1 (AP, −2 mm; ML, −1.6 or +1.6 mm; DV, −1.6 mm) and a 5 μl hamilton needle loaded with AAV was introduced slowly by using a syringe pump. 0.3 μl of virus was injected bilaterally at a rate of 0.05 μl/min. After a 10 minutes delay, the needle was pulled up. Electrophysiological recordings and behavior experiments were performed 28 days after viral transduction. The CamkII Cre virus were generated by BrainVTA (Wuhan, China).

Intracerebral Infusions
The mice were anesthetized with 1% pentobarbital sodium and placed in a stereotaxic frame. The scalp was incised and a hole drilled into the skull above the hippocampus CA1 (AP, −2 mm; ML, −1.6 or +1.6 mm; DV, −1.6 mm). Stainless-steel guide cannulas (RWD; 62004; length, 2 mm) were lowered into the dorsal hippocampal CA1. The guide cannulas were secured in place using glass ionomer cements. Dummy cannulas (RWD; 62104, with lengths matching the guide cannulas) were placed inside the guide cannulas to prevent occlusion. Incisions were fixed and covered with glass ionomer cement. The animals were removed from the stereotaxic instrument and recovered on an electric blanket, and then they were placed back into their home cages. The infusion of CDPPB or ACSF was performed 7 days after surgery and behavior tests were performed 30 min after infusion. The dummy cannulas were removed from the guide cannulas and replaced by infusion cannulas (RWD; 62204). The infusion cannulas were connected, via polyethylene tubing (RWD; BC-22) to 5 μl microsyringes (Hamilton, Reno, NV) mounted on a microinfusion pump (RWD200, China). Each mouse was injected with 0.3 μl/side at a flow rate of 0.1 μl/min. To allow the diffusion of the drug, the infusion cannulas were kept in for 3 min before being replaced with the dummy cannulas.

Slice for confocal microscopy
Mice, microinjected with AAV-CamKII-GFP or AAV-CamKII-Cre, were anesthetized and perfused transcardially with 4% paraformaldehyde in 0.1 M PBS (pH 7.4). Brains were post-fixed overnight in the same solution, and then stored in 30% sucrose (wt/vol) in PBS. All brains were cut into 40 μm coronal sections on a cryostat. A series of fluorescent images were obtained with the A1 Nikon confocal microscope.

Open field test
The open-field apparatus was a rectangular chamber (60 × 60 × 40 cm) that was composed of gray polyvinyl chloride. The center area was illuminated using 25 W halogen bulbs (200 cm above the field). The mice were gently placed into the center of the testing chamber for a 5 min recording period and monitored using an automated video tracking system. The digitized image of the path taken in those 5 min was automatically analyzed using the DigBehv animal behavior analysis program.

Elevated plus maze test
The elevated plus maze test comprised two open arms (10 × 50 cm) located opposite one another and two opposing enclosed arms (10 × 50 × 40 cm) 40 cm above the floor. The junction of the four arms(the central platform) measured 10 × 10 cm. All experimental mice were taken to a dimly lit testing room 30 min prior to the test. At the beginning of the 5 min test, the mice were placed onto the central platform of the elevated plus-maze facing the closed arm. The maze was cleaned between the sessions using 70% ethanol. We used computational software to automatically quantify the time spent and distance travelled in the closed and open arms.

Statistical analyses
Statistical analysis was conducted using GraphPad Prism version 7.0 (GraphPad Software). All data are expressed as the mean ± SEM. Student's t-test was used to compare the data from two groups. One-way ANOVA was used for the analysis of data from three or more groups. Two-way ANOVA was used in analyzing more than two parameters. In the cumulative frequency distribution curves of EPSC/ IPSC frequency, the bin-widths were 100 ms across all experiments. In the cumulative frequency distribution curves of EPSC/ IPSC amplitude, the bin-widths were 2 pA across all experiments. The statistical significance level for all experiments was set at $P < 0.05$.

RESULTS
Chronic restraint stress leaded to anxiety-like behaviors and reduced glutamatergic and GABAergic inputs in hippocampal CA1 pyramidal neurons
To understand the underlying mechanism how chronic stress induces anxiety-like behavior, chronic restraint stress (CRS) model was adopted in this study. Mice were subjected to a 5-day restraint stress for 2 h per day in a well-ventilated Perspex tube and then underwent two anxiety-related behavioral tests, open

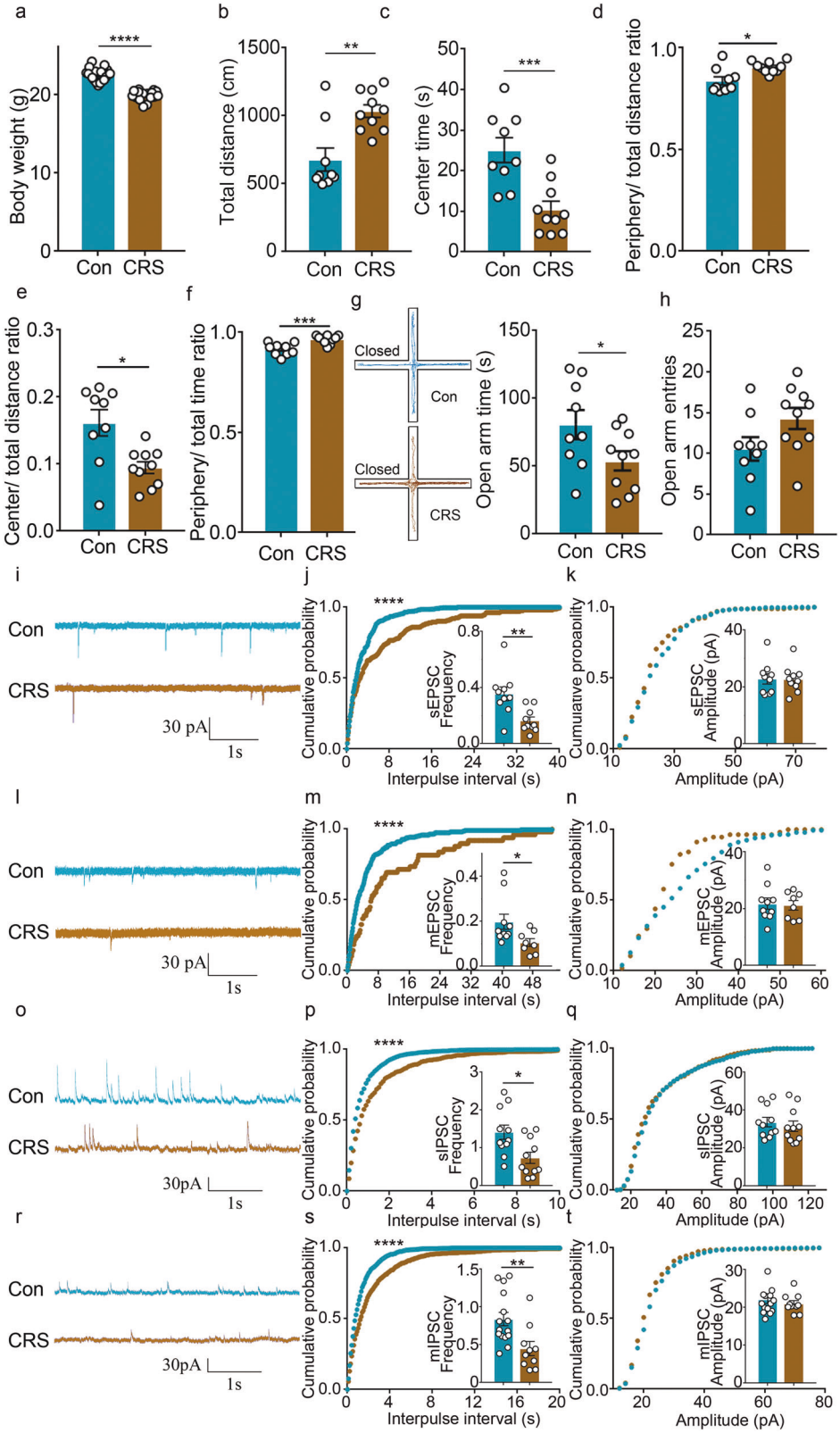

field test and elevated plus maze [24]. As reported, we found that mice exposed to restraint stress showed decreased weight, traveled more distance and spent less time in the central area in open field test (Fig. 1a–c) [25]. The periphery/ center distance ratio and periphery time ratio can be used as an indicator for anxiety-related responses. We found that mice exposed to restraint stress traveled a significantly higher proportion of distance and time in the periphery, and lower proportion of distance in the center, indicating an increased anxiety-like behavior after CRS (Fig. 1d–f). Moreover, the mice exposed to

Fig. 1 Chronic restraint stress leaded to anxiety-like behaviors and impaired the synaptic inputs in hippocampal CA1 pyramidal neurons. **a** After 5 days of chronic restraint stress, the weight of the mice was decreased. $n = 19$ mice for control group, $n = 18$ mice for chronic restraint stress group. ****$P < 0.0001$ by two-tailed unpaired Student's t-test. $t = 11.15$, d.f. = 35. **b–f** After 5 days of chronic restraint stress, the mice showed increased locomotion and anxiety-like behavior in the open field test. $n = 9$ mice for control group, $n = 10$ mice for chronic restraint stress group. Total distance: **$P < 0.01$ by two-tailed unpaired Student's t-test. $P = 0.0015$, $t = 3.782$, d.f. = 17. Center time: ***$P < 0.001$ by two-tailed unpaired Student's t-test. $P = 0.0008$, $t = 4.078$, d.f. = 17. Periphery/ total distance ratio: *$P < 0.05$ by two-tailed Mann Whitney test. $P = 0.0101$. Center/ total distance ratio: *$P < 0.05$ by two-tailed Mann Whitney test. $P = 0.0101$. Periphery/ total time ratio: ***$P < 0.001$ by two-tailed unpaired Student's t-test. $P = 0.0008$, $t = 4.078$, d.f. = 17. **g**, **h** After 5 days of chronic restraint stress, the mice decreased open arm time in the elevated plus maze test. No difference in open arm entries. $n = 9$ mice for control group, $n = 10$ mice for chronic restraint stress group. Open arm time: *$P < 0.05$ by two-tailed unpaired Student's t-test. $P = 0.0495$, $t = 2.115$, d.f. = 17. **i–k** Representative traces and quantitative analysis of sEPSC. $n = 10$ cells from 4 mice in the control group, $n = 10$ cells from 3 mice in the CRS group. **$P < 0.01$ by two-tailed unpaired Student's t-test. $P = 0.003$, $t = 3.425$, d.f. = 18. ****$P < 0.0001$ by Kolmogorov-Smirnov test. Scale bar: 1 s, 30 pA. **l–n** Representative traces and quantitative analysis of mEPSC. $n = 10$ cells from 4 mice in the control group, $n = 8$ cells from 4 mice in the CRS group. *$P < 0.05$ by two-tailed unpaired Student's t-test. $P = 0.0386$, $t = 2.254$, d.f. = 16. Cumulative probability: ****$P < 0.0001$ by Kolmogorov-Smirnov test. Scale bar: 1 s, 30 pA. **o–q** Representative traces and quantitative analysis of sIPSC. $n = 11$ cells from 4 mice for each group. *$P < 0.05$ by two-tailed unpaired Student's t-test. $P = 0.0107$, $t = 2.813$, d.f. = 20. ****$P < 0.0001$ by Kolmogorov-Smirnov test. Scale bar: 1 s, 30 pA. **r–t** Representative traces and quantitative analysis of mIPSC. $n = 15$ cells from 4 mice in the control group, $n = 10$ cells from 4 mice in the CRS group. **$P < 0.01$ by two-tailed unpaired Student's t-test. $P = 0.007$, $t = 2.963$, d.f. = 23. Cumulative probability: ****$P < 0.0001$ by Kolmogorov-Smirnov test. Scale bar: 1 s, 30 pA. Error bars, mean ± SEM.

restraint stress spent less time in the open arms in elevated plus maze, while no significant difference was found in open arm entries (Fig. 1g, h). In summary, these results indicated that chronic restraint stress induced anxiety-like behavior.

Structural degeneration in hippocampus have been reported in the pathogenesis of anxiety, which support an important role of the hippocampus in anxiety [26]. To investigate the cellular mechanism underlying chronic stress induced anxiety-like behavior, we conducted electrophysiological recordings in hippocampal CA1 pyramidal neurons of chronic stressed mice. To determine whether chronic restraint stress could modify excitatory synaptic inputs, sEPSCs and mEPSCs were recorded. The mean values of sEPSC and mEPSC frequency were decreased after CRS, while no change was found on the mean values of sEPSC or mEPSC amplitude between the groups (Fig. 1i–n). In the cumulative frequency distribution curves, Kolmogorov-Smirnov (KS) test revealed a significant decrease in sEPSC and mEPSC frequency of CA1 pyramidal neurons after CRS. These results indicate that chronic restraint stress impaired excitatory synaptic inputs.

Next, to test whether chronic restraint stress could modify inhibitory synaptic inputs, sIPSCs and mIPSCs were recorded in CA1 pyramidal neurons. The mean values of sIPSC and mIPSC frequency were decreased after chronic restraint stress, while no change was found on the mean values of sIPSC or mIPSC amplitude between the groups (Fig. 1o–t). In the cumulative frequency distribution curves, Kolmogorov-Smirnov (KS) test revealed a significant decrease in sIPSC and mIPSC frequency of CA1 pyramidal neurons after CRS. Together, these results indicated that chronic restraint stress also impaired inhibitory synaptic inputs. Considering that chronic restraint stress mainly decreased mEPSC and mIPSC frequencies, but not the amplitude, these results suggested that impaired synaptic transmission might be due to a presynaptic mechanism.

Chronic restraint stress decreased mGluR5 expression in hippocampal CA1 and mGluR5 knockdown produced anxiety-like behaviors

To test whether mGluR5 in hippocampus was involved in anxiety-like behaviors, we studied chronic restraint stress induced mGluR5 regulation in hippocampal CA1, CA3 and DG using quantitative PCR. Remarkably, we found that mGluR5 in CA1 was down-regulated after chronic restraint stress, but not in CA3 or DG (Fig. 2a–c). Then, the expression of mGluR5 in CA1 was decreased compared with the control mice when detected by Wes (Fig. 2d). These results suggested that mGluR5 in hippocampal CA1 might be involved in the anxiety-like behaviors induced by chronic restraint stress.

We then examined whether knockdown of mGluR5 in hippocampal CA1 pyramidal neurons by AAV-CamkII-Cre has effect on anxiety-like behavior. To validate the selectivity of mglur5 deletion, we microinjected AAV-CamkII-Cre-EGFP into the hippocampus of Ai14 mice and found that EGFP and Cre were mainly expressed in hippocampal CA1 pyramidal neurons (Fig. 2e, f). Next, we microinjected AAV-CamkII-EGFP or AAV-CamkII-Cre-EGFP into the hippocampus of mGluR5 loxP/loxP mice. Four weeks later, the expression of mGluR5 was significantly decreased in the AAV-CamkII-Cre injected mice when detected by quantitative PCR and Wes (Fig. 2g, h).

Next, the mice underwent tests for anxiety-like behavior. In open field test, we found that AAV- CamkII-Cre injected mice traveled less distance and spent less time in the central area when compared with AAV-CamkII-GFP injected mice (Fig. 2i, j). Meanwhile, we found that AAV-CamkII-Cre injected mice traveled a significantly higher proportion of distance and time in the periphery, and lower proportion of distance in the center, indicating an increased anxiety-like behavior after mGluR5 knockdown (Fig. 2k–m). Furthermore, the AAV-CamkII-Cre injected mice spent less time and had less open arm entries in the open arms (Fig. 2n, o). Together, these results indicated that knockdown of mGluR5 in hippocampal CA1 pyramidal neurons produced anxiety-like effects.

Knockdown of mGluR5 in hippocampal CA1 pyramidal neurons mainly inhibited the GABAergic inputs

To understand the cellular mechanism underlying knockdown of mGluR5 in hippocampal CA1 pyramidal neurons induced anxiety-like behavior, we conducted electrophysiological recording on AAV-CamkII-GFP and AAV-CamkII-Cre injected mice. To determine whether knockdown of mGluR5 in hippocampal CA1 could modify excitatory synaptic inputs, sEPSCs and mEPSCs were recorded in CA1 pyramidal neurons. Our data showed that the frequency of sEPSCs/ mEPSCs were significantly altered when tested on the cumulative curves by KS test, but a nonsignificant trend when tested on the mean values (Fig. 3a–f). These results indicated that knockdown of mGluR5 in CA1 pyramidal neurons inhibited excitatory synaptic inputs.

Next, to test whether knockdown of mGluR5 in hippocampal CA1 could modify inhibitory synaptic inputs, sIPSCs and mIPSCs were recorded in CA1 pyramidal neurons. We found that the mean values of sIPSC and mIPSC frequency was significantly decreased when compared with the control group, while no change was found on the mean values of sIPSC or mIPSC amplitude between the groups (Fig. 3g–l). In the cumulative frequency distribution curves, KS test revealed a significant decrease in sIPSC and mIPSC frequency of CA1 pyramidal neurons after mGluR5 knockdown,

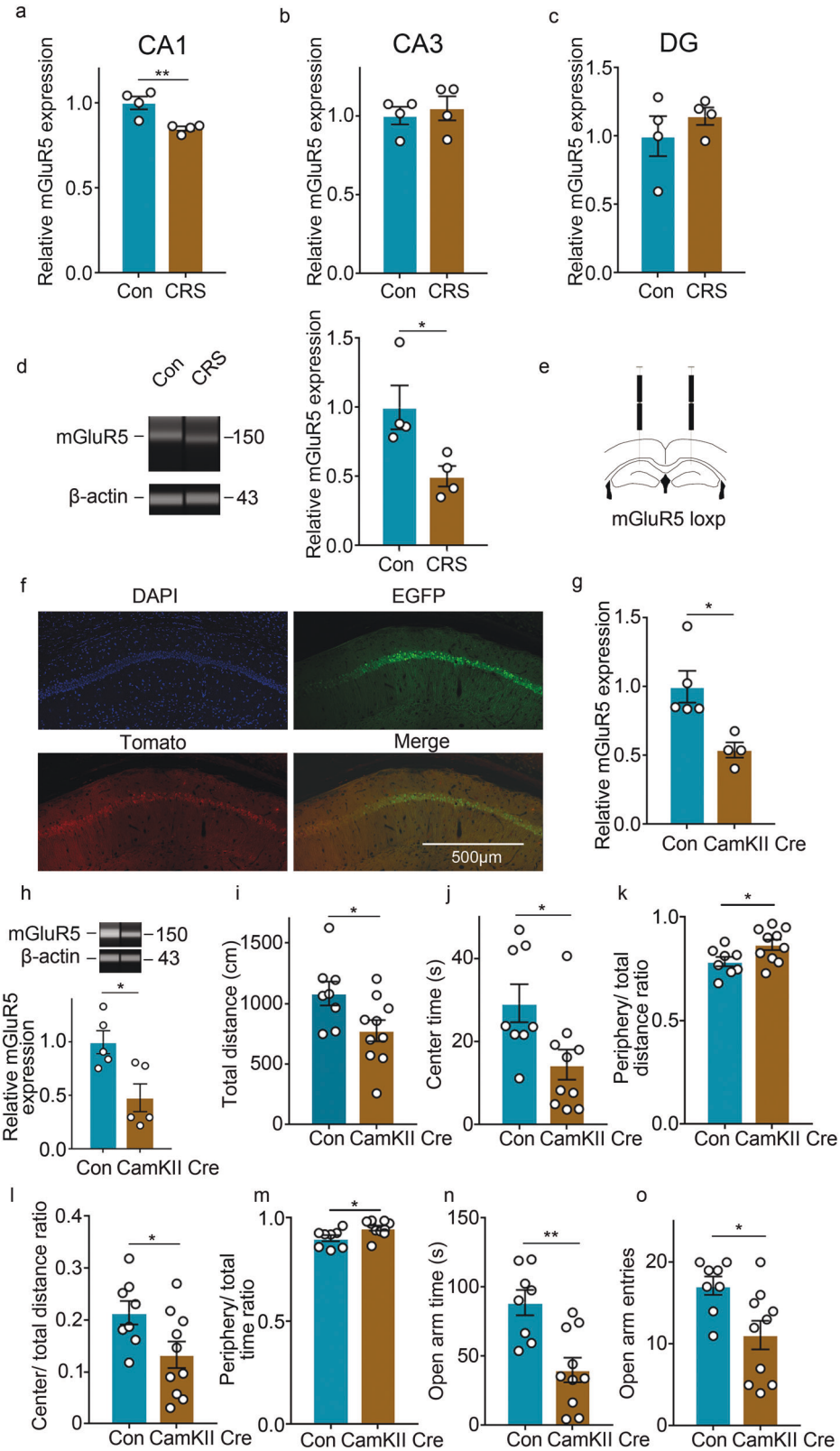

indicating that knockdown of mGluR5 impaired inhibitory synaptic inputs. Notably, the decreased extent in sIPSC and mIPSC frequency was larger than that in sEPSC and mEPSC frequency. Therefore, these results suggested that mGluR5 knockdown mainly impaired inhibitory synaptic inputs.

The positive allosteric modulator of mGluR5 restored impaired inhibitory synaptic inputs after chronic stress

CDPPB, a positive allosteric modulator of mGluR5, could potentiate the activity of mGluR5. Previous studies suggested that CDPPB could rescue the decreased mEPSC frequency in neurons knocked

Fig. 2 Chronic restraint stress decreases mGluR5 expression in hippocampal CA1 and mGluR5 knockdown produced anxiety-like behaviors. a–c mGluR5 in CA1 was downregulated after chronic restraint stress. No difference in CA3 or DG. $n = 4$ mice for each group. CA1: $^{**}P < 0.01$ by two-tailed unpaired Student's t-test. $P = 0.0086$, $t = 3.84$, d.f. = 6. **d** Western analysis of mGluR5 expression after chronic restraint stress. $n = 4$ mice for each group. $^{*}P < 0.05$ by two-tailed unpaired Student's t-test. $P = 0.0295$, $t = 2.842$, d.f. = 6. **e** The diagram of virus injected sites. **f** Representative images of the distribution of AAV injected mice. Scale bar: 500 μm. **g** qPCR analysis of mGluR5 expression in AAV-CamKII-Cre injected mice. $n = 5$ mice for control group, $n = 4$ mice for AAV-CamKII-Cre group. $^{*}P < 0.05$ by two-tailed unpaired Student's t-test. $P = 0.0134$, $t = 3.285$, d.f. = 7. **h** Western blot analysis of mGluR5 expression after AAV-CamKII-Cre injection. $n = 5$ mice for each group. $^{*}P < 0.05$ by two-tailed unpaired Student's t-test. $P = 0.0148$, $t = 3.095$, d.f. = 8. **i–m** The AAV-CamKII-Cre injected mice showed decreased locomotion and increased anxiety-like behavior in the open field test. n = 8 mice for control group, $n = 10$ mice for AAV-CamKII-Cre group. Total distance: $^{*}P < 0.05$ by two-tailed unpaired Student's t-test. $P = 0.0334$, $t = 2.328$, d.f. = 16. Center time: $^{*}P < 0.05$ by two-tailed unpaired Student's t-test. $P = 0.0207$, $t = 2.567$, d.f. = 16. Periphery/ total distance ratio: $^{*}P < 0.05$ by two-tailed unpaired Student's t-test. $P = 0.0338$, $t = 2.321$, d.f. = 16. Center/ total distance ratio: $^{*}P < 0.05$ by two-tailed unpaired Student's t-test. $P = 0.0338$, $t = 2.321$, d.f. = 16. Periphery/ total time ratio: $^{*}P < 0.05$ by two-tailed unpaired Student's t-test. $P = 0.0207$, $t = 2.567$, d.f. = 16. **n**, **o** The AAV-CamKII-Cre injected mice showed decreased open arm time, open arm entries in the elevated plus maze test. $n = 8$ mice for control group, $n = 10$ mice for AAV-CamKII-Cre group. Open arm time: $^{**}P < 0.01$ by two-tailed unpaired Student's t-test. $P = 0.0016$, $t = 3.794$, d.f. = 16. Open arm entries: $^{*}P < 0.05$ by two-tailed unpaired Student's t-test. $P = 0.0145$, $t = 2.74$, d.f. = 16. Error bars, mean ± SEM.

down for Shank3 and could reverse the whisker deprivation-induced PPR increase [27, 28]. Thus, we investigated whether 5 μM CDPPB could restore the decreased GABAergic inputs after chronic stress. sIPSCs was recorded in CA1 pyramidal neurons. We found that CDPPB increased the mean values of sIPSCs frequency when compared with vehicle controls in chronic stressed group, while no change was found in the mean values of sIPSCs amplitude between the groups (Fig. 4a–c). Meanwhile, △sIPSC frequency was increased after CDPPB application in the CRS group, while no significant difference was observed in the control group (Fig. 4d, e). KS test of the cumulative frequency distribution curves also revealed a significant rescue in sIPSC frequency. Together, these results indicated that CDPPB application could restore the impaired inhibitory synaptic inputs after chronic stress.

Similarly, mIPSCs was recorded in CA1 pyramidal neurons and we found that the mean value of mIPSC frequency was restored after CDPPB application in the CRS group, while no significant difference was observed in the control group (Fig. 4f–h). Meanwhile, △mIPSC frequency was increased after CDPPB application in the CRS group, while no significant difference was observed in the control group (Fig. 4i, j). KS test of the cumulative frequency distribution curves also revealed a significant rescue in mIPSC frequency. Together, these results indicated that CDPPB application could restore the impaired inhibitory synaptic inputs after chronic stress.

The positive allosteric modulator of mGluR5 restored stress-induced anxiety-like behavior

Next, we examined the effect of CDPPB on stress-induced anxiety-like behavior. Mice were intraperitoneally injected with 5 mg/kg CDPPB after 5 days of restraint stress and underwent anxiety-related behavioral tests. In the open field test, injection of CDPPB did not restore the proportion of time and distance in the center and in the periphery (Fig. 5a–e). In the elevated plus maze test, injection of CDPPB restored the number of entries into open arms and time spent in open arms (Fig. 5f–h). Meanwhile, the control mice did not show significant difference in locomotion or anxiety-like behavior after CDPPB application (supplementary Fig. S1). Therefore, our results suggested that CDPPB could partially rescue stress-induced anxiety disorders.

Given that mGluR5 is widely expressed in the brain, we locally infused CDPPB into dorsal hippocampal CA1 region in mice subjected to CRS to test whether this treatment could restore the heightened anxiety-like behavior. In the open field test, local infusion of CDPPB in the dorsal CA1 did not rescue stress-induced anxiety-like behavior (Fig. 5i–n). However, in the elevated plus maze test, injection of CDPPB restored time spent in open arms (Fig. 5o, p). Moreover, local injection of CDPPB also had no effect on anxiety-like behaviors in control mice (Fig. 5j–p). In summary, our results suggested that local infusion of CDPPB into hippocampal CA1 region could partially rescue stress-induced anxiety disorders.

DISCUSSION

In this study, we found that the low expression of mGluR5 in hippocampal CA1 was associated with anxiety-like behaviors in chronic restraint stress model. Knockdown of mGluR5 in hippocampal CA1 induced anxiety-like behavior. Chronic restraint stress reduced the inhibitory synaptic inputs in hippocampal CA1 pyramidal neurons. Meanwhile, knockdown of mGluR5 also decreased inhibitory synaptic inputs in hippocampal CA1 pyramidal neurons. Finally, we also found that CDPPB restored the decreased inhibitory synaptic inputs and increased anxiety-like behavior after chronic restraint stress (Fig. 5q).

Chronic restraint stress, a typical animal model for stress disorders, has been shown to elicit behavioral, gene expression and synaptic transmission changes similar to the patients under stress [29–32]. However, no study to date has clarified the association between mGluR5 and chronic restraint stress. Some studies showed that the mGluR5 protein levels are not altered in response to restraint stress, in which they dissected the whole hippocampus [33]. Our results found that the expression of mGluR5 was decreased in hippocampal CA1 after the chronic restraint stress, but unaltered in hippocampal CA3 or DG. Therefore, it is important to determine the mGluR5 protein levels in different subregions of the hippocampus. Extensive research has identified a critical role of mGluR5 in learning and memory [34–36]. However, little is known about the role of mGluR5 in stress-induced anxiety-like behavior. Through targeted pharmacological manipulation, our previous study indicated that mGluR5 in BLA regulates anxiety-like behavior after social isolation [13]. Considering that pharmacological manipulation could not decipher the function of mGluR5 in a cell-type-specific manner, we used AAV-CamKII-Cre to knockdown mGluR5 in hippocampal CA1 pyramidal neurons. Our results provide an important role of mGluR5 in regulating anxiety-like behaviors.

Hippocampus is known to be essential for cognitive processes and anxiety disorders [37]. Previous study suggested that "anxiety cells" are more abundant in ventral CA1 than in dorsal CA1 and neural activity in the ventral CA1 is correlated with anxiety-like behaviors in rodents [23]. However, they did not explore whether dorsal CA1 could regulate anxiety-like behaviors. Their data are mainly correlation analysis, which is lack of interventions in dorsal CA1. Besides our results, many previous studies have showed that dorsal CA1 is implicated in regulating anxiety-like behaviors [20, 38, 39]. It has been found that median raphe serotonin neurons promote anxiety-like behavior via inputs to the dorsal hippocampus [20]. Moreover, the researchers found that

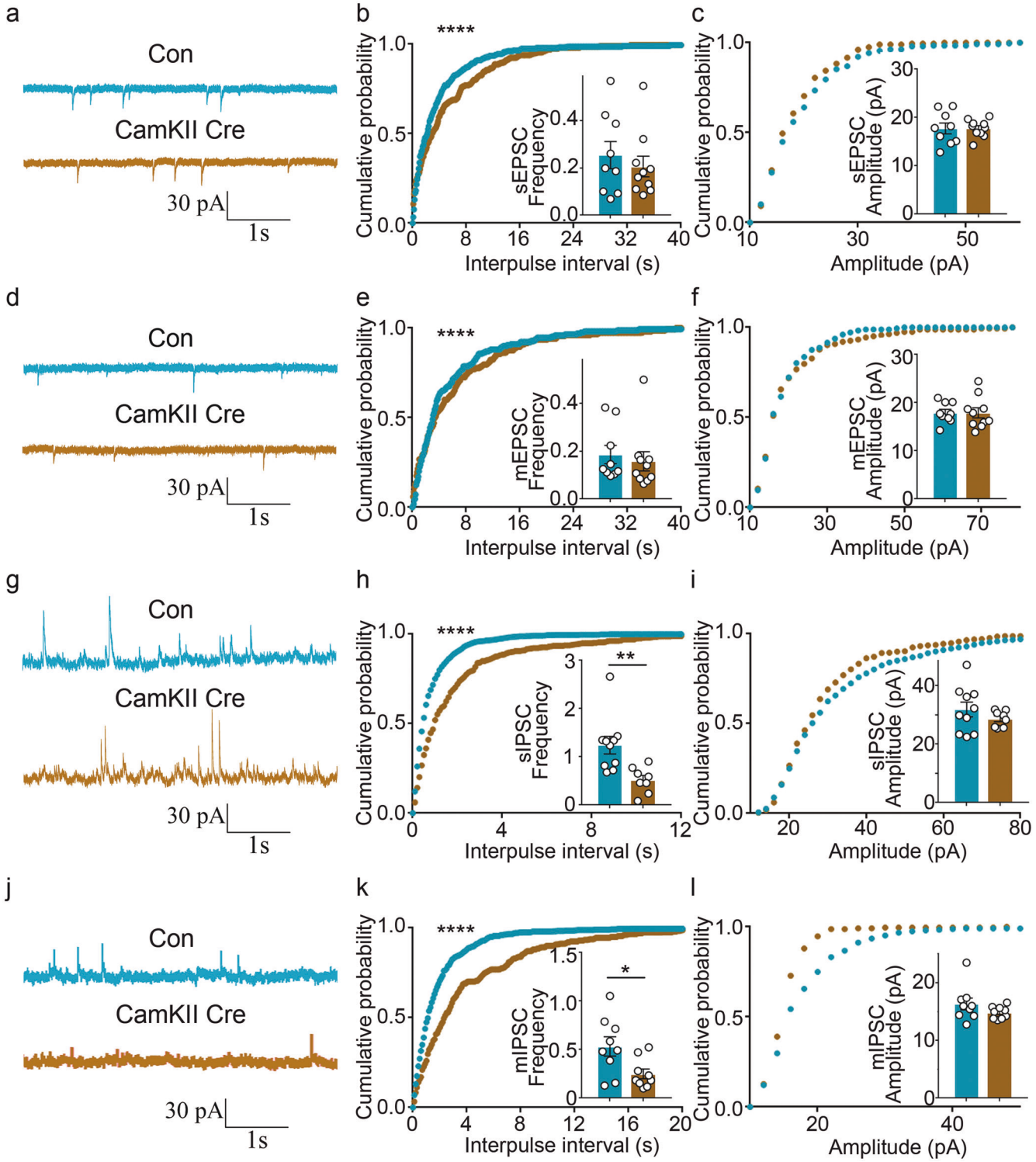

Fig. 3 Knockdown of mGluR5 in hippocampal CA1 pyramidal neurons impairs inhibitory synaptic inputs. a–c Representative traces and quantitative analysis of sEPSC. $n = 9$ cells from 4 mice in the control group, $n = 10$ cells from 4 mice in the AAV-CamkII-Cre group. Cumulative probability: $^{****}P < 0.0001$ by Kolmogorov-Smirnov test. Scale bar: 1 s, 30 pA. **d–f** Representative traces and quantitative analysis of mEPSC. $n = 9$ cells from 4 mice in the control group, $n = 10$ cells from 4 mice in the AAV-CamkII-Cre group. Cumulative probability: $^{****}P < 0.0001$ by Kolmogorov-Smirnov test. Scale bar: 1 s, 30 pA. **g–i** Representative traces and quantitative analysis of sIPSC. $n = 10$ cells from 4 mice in the control group, $n = 8$ cells from 4 mice in the AAV-CamkII-Cre group. $^{**}P < 0.01$ by two-tailed unpaired Student's t-test. $P = 0.0049$, $t = 3.259$, d.f. = 16. $^{****}P < 0.0001$ by Kolmogorov-Smirnov test. Scale bar: 1 s, 30 pA. **j–l** Representative traces and quantitative analysis of mIPSC. $n = 9$ cells from 4 mice in each group. $^{*}P < 0.05$ by two-tailed unpaired Student's t-test. $P = 0.0216$, $t = 2.545$, d.f. = 16. $^{****}P < 0.0001$ by Kolmogorov-Smirnov test. Scale bar: 1 s, 30 pA. Error bars, mean ± SEM.

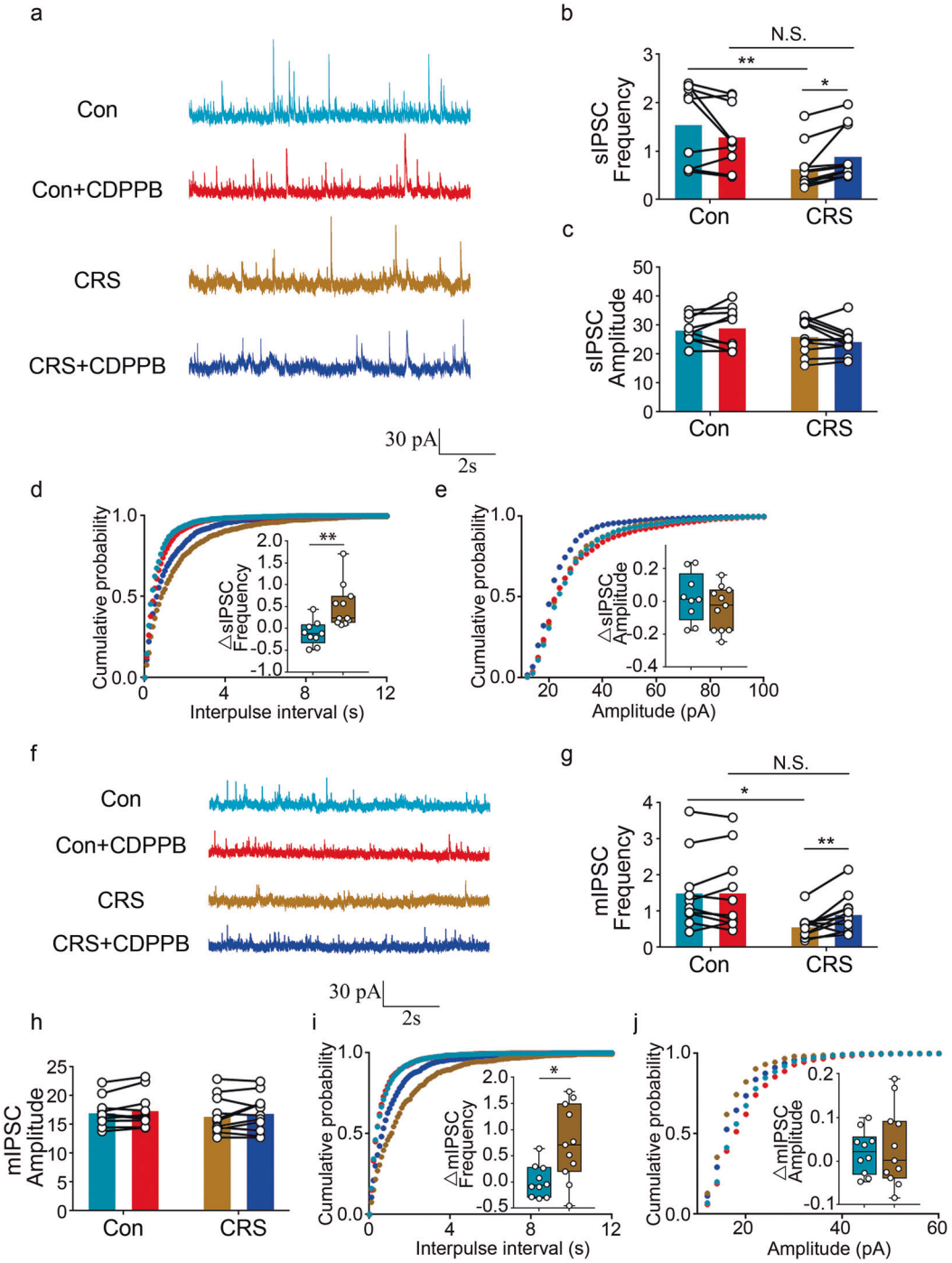

Fig. 4 The CDPPB restored stress-impaired inhibitory synaptic inputs. a Representative traces of sIPSCs. Scale bar: 2 s, 30 pA. **b**, **c** Quantitative analysis of sIPSCs after CDPPB application. sIPSC frequency: $n = 9$ cells from 4 mice in the control group, $n = 11$ cells from 4 mice in the CRS group. $^{*}P < 0.05$, $^{**}P < 0.01$ by Repeated measure two-way ANOVA. Con(before) versus CRS(before): $P = 0.0048$. CRS(before) versus CRS(after): $P = 0.0366$. Con(before) versus CRS(after): $P = 0.1037$. No difference in sIPSC amplitude. **d**, **e** Quantitative analysis of △sIPSC after CDPPB application. △sIPSC frequency was calculated by (f2 - f1)/f1, where f1 and f2 were the frequencies of sIPSCs recorded before and after CDPPB treatment, respectively. △sIPSC amplitude was calculated by (a2 - a1)/a1, where a1 and a2 were the amplitudes of sIPSCs recorded before and after CDPPB treatment, respectively. △sIPSC frequency: $n = 9$ cells from 4 mice in the control group, $n = 11$ cells from 4 mice in the CRS group. $^{**}P < 0.01$ by two-tailed unpaired Student's t-test. $P = 0.0042$. No difference in △sIPSC amplitude. Cumulative frequency distribution curves of sIPSC frequency: Con versus CRS: $^{****}P < 0.0001$ by Kolmogorov-Smirnov test. CRS versus CRS + CDPPB: $P = 0.0188$ by Kolmogorov-Smirnov test. **f** Representative traces of mIPSCs. Scale bar: 2 s, 30 pA. **g**, **h** Quantitative analysis of mIPSCs after CDPPB application. mIPSC frequency: $n = 10$ cells from 4 mice in the control group, $n = 11$ cells from 4 mice in the CRS group. $^{*}P < 0.05$, $^{**}P < 0.01$ by Repeated measure two-way ANOVA. Con(before) versus CRS(before): $P = 0.0217$. CRS(before) versus CRS(after): $P = 0.0046$. Con(before) versus CRS(after): $P = 0.4639$. No difference in mIPSC amplitude. **i**, **j** Quantitative analysis of △mIPSC after CDPPB application. △mIPSC frequency: $n = 10$ cells from 4 mice in the control group, $n = 11$ cells from 4 mice in the CRS group. $^{*}P < 0.05$ by Mann-Whitney test. $P = 0.0127$. No difference in △mIPSC amplitude. Cumulative frequency distribution curves of mIPSC frequency: Con versus CRS: $^{****}P < 0.0001$ by Kolmogorov-Smirnov test. CRS versus CRS + CDPPB: $^{****}P < 0.0001$ by Kolmogorov- Smirnov test. Error bars, mean ± SEM.

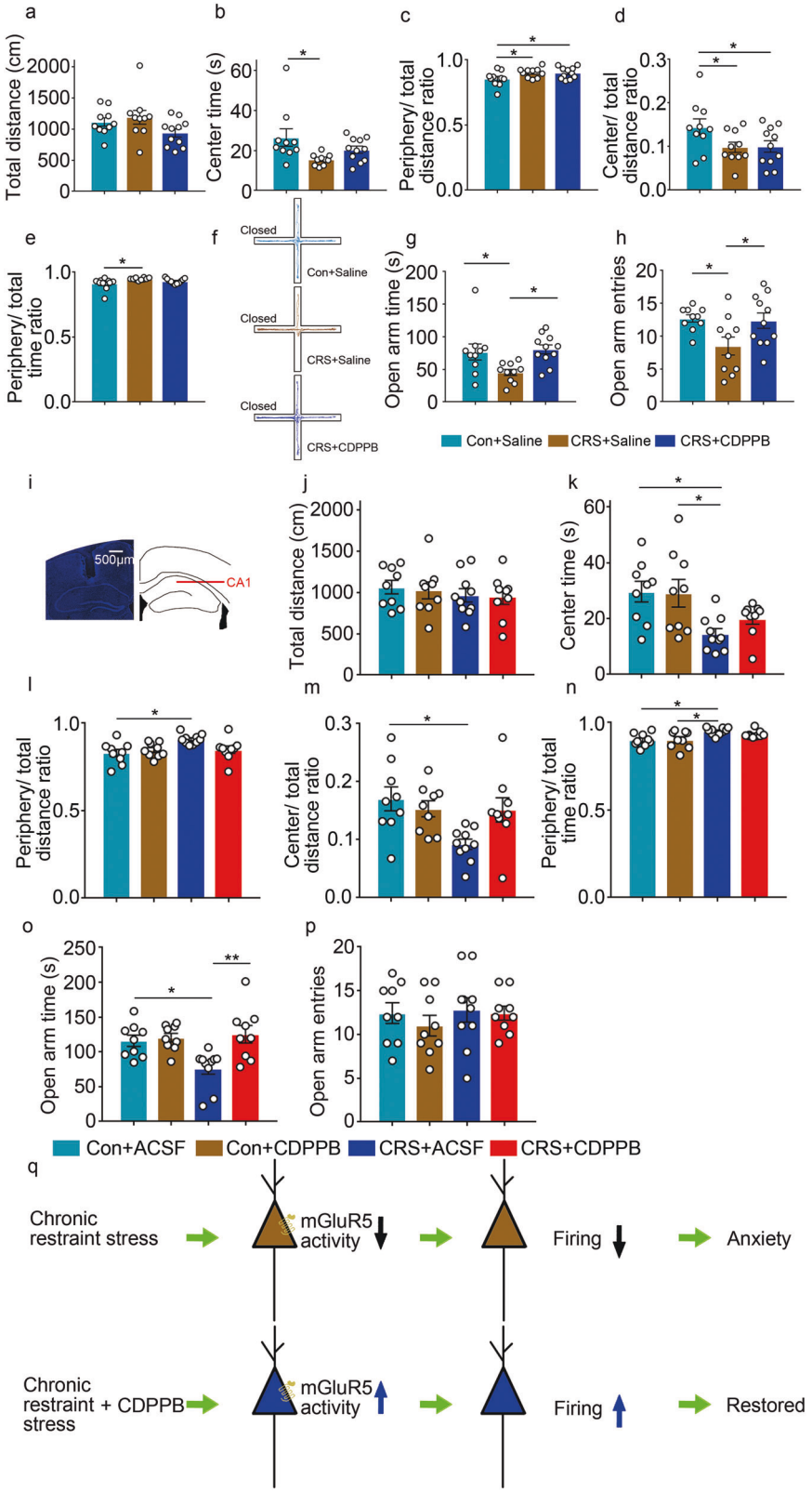

hippocampal HCN1 channels or Lrp4 in dorsal CA1 could regulate anxiety-like behaviors [38, 39]. There were some researches investigating inhibitory synaptic inputs in the hippocampus after chronic restraint stress and the results were complicated. Some researches showed that chronic restraint stress suppressed inhibitory synaptic inputs in hippocampal pyramidal neurons [40, 41], while other researches suggested that chronic restraint stress facilitated inhibitory synaptic inputs in hippocampal pyramidal neurons [42]. The contradiction might be due to the days and hours per day spent in restraint stress.

Fig. 5 The CDPPB restored stress-induced anxiety-like behavior. a–e The CDPPB did not rescue stress-induced anxiety-like behavior in the open field test. $n = 10$ mice for control group, $n = 10$ mice for CRS group, $n = 11$ mice for CRS + CDPPB group. **f** Representative traces in elevated plus maze test after CDPPB treatment. **g, h** The CDPPB treated mice showed restored open arm time and open arm entries in the elevated plus maze test. $n = 10$ mice for control group, $n = 10$ mice for CRS group, $n = 11$ mice for CRS + CDPPB group. Open arm time: $^*P < 0.05$ by One-way ANOVA, $F_{2,28} = 5.169$. Con versus CRS: $P = 0.0397$, $q = 3.648$, d.f. = 28. CRS versus CRS + CDPPB: $P = 0.0162$, $q = 4.199$, d.f. = 28. Open arm entries: $^*P < 0.05$ by One-way ANOVA. $F_{2,28} = 4.447$. Con versus CRS: $P = 0.0326$, $q = 3.772$, d.f. = 28. CRS versus CRS + CDPPB: $P = 0.0461$, $q = 3.552$, d.f. = 28. **i** Representative infusion site (as indicated by the arrow) in the mouse dorsal hippocampal CA1 area. **j–n** Local infusion of CDPPB in dorsal CA1 did not rescue stress-induced anxiety-like behavior in the open field test. $n = 9$ mice for control group, $n = 9$ mice for Con+CDPPB group, $n = 10$ mice for CRS group, $n = 9$ mice for CRS + CDPPB group. Center time: $^*P < 0.05$ by Two-way ANOVA. Con versus CRS: $P = 0.0145$, $t = 3.284$, d.f. = 33. Con+CDPPB versus CRS: $P = 0.0206$, $t = 3.15$, d.f. = 33. **o, p** Local infusion of CDPPB in dorsal CA1 rescued reduced open arm time, but not open arm entries, in the elevated plus maze test. $n = 9$ mice for control group, $n = 9$ mice for Con+CDPPB group, $n = 10$ mice for CRS group, $n = 9$ mice for CRS + CDPPB group. Open arm time: $^*P < 0.05$, $^{**}P < 0.01$ by Two-way ANOVA. Con versus CRS: $P = 0.0196$, $t = 3.1$, d.f. = 33. CRS versus CRS + CDPPB: $P = 0.0033$, $t = 3.83$, d.f. = 33. **q** Schematic diagram of the involvement of mGluR5 in the hippocampus in anxiety-like behavior. Chronic restraint stress decreases mGluR5 activity in the hippocampus, leading to deficits of firing and the development of anxiety-like behavior. CDPPB reversed the chronic restraint stress-induced decrease in firing in the hippocampus and chronic restraint stress-induced increase in anxiety-like behavior. Error bars, mean ± SEM.

In mGluR5 knockdown mice, the reduced extent in sIPSC and mIPSC frequency was larger than that in sEPSC and mEPSC frequency. Therefore, these results suggested that mGluR5 knockdown mainly impaired inhibitory synaptic inputs. One possible reason for this is that there may be retrograde signal from postsynaptic side to affect GABAergic presynaptic vesicles release. Previous studies showed that inhibition of mGluR5 could upregulate hippocampal BDNF levels [43, 44]. Postsynaptic BDNF could act as a retrograde synaptic regulator to reduce GABAergic input [45]. Therefore, it might be the elevated BDNF after mGluR5 knockdown that was responsible for the impaired GABAergic presynaptic vesicles release.

Previous study also showed that restraint stress bidirectionally modulates excitatory synaptic inputs in the hippocampus, in which restraint stress decreased the frequency of spontaneous excitatory currents after three repetitions but enhanced it after 14 and 21 repetitions [46]. Our results suggested that excitatory synaptic inputs in the hippocampus was decreased after 5-day chronic restraint stress. However, the reduced extent was less in mGlur5 KD mice (Fig. 3b, e) than in CRS mice (Fig. 1j, m). Given that CRS could affect many brain regions, other brain regions (besides hippocampal CA1) might be also implicated in the decreased excitatory synaptic inputs into hippocampus.

In previous studies, the mGluR5 activation induced significant increase in IPSC frequency [47, 48], which suggested that mGluR5 could modify inhibitory synaptic inputs. CDPPB, a positive allosteric modulator of mGluR5, could potentiate the activity of mGluR5. Previous studies showed that CDPPB could alleviate the anxiety-like behavior in the open field and hypersociability in the three-chamber test [49]. Thus, in our study, it is possible that the decreased inhibitory synaptic inputs after mGluR5 knockdown contributes to the facilitation of anxiety-like behaviors. CDPPB has been shown to be brain-penetrant and thus might be a potential therapeutic drug to treat anxiety disorders.

mGluR5 is known to be important for regulating a variety of ion channels and NMDA receptors, leading to the alteration of firing rate and neuronal excitability. Using mGluR5 KO mice, previous work indicated that mGluR5-dependent Ca^{2+} was necessary for high-frequency stimulations-induced increase in dendritic $I_{Na,P}$, which leaded to the enhanced probability of AP firing [50]. It has also been reported that activation of group I mGluRs including mGluR5 increases calcium release from intracellular stores and leads to cell depolarization and enhanced excitability [51]. Moreover, the activity of pyramidal cells in hippocampal CA1 could regulate anxiety-like behaviors [20, 52]. Thus, in our study, it is possible that the decreased excitability and firing of CA1 pyramidal neurons after mGluR5 knockdown might also contribute (plus reduced synaptic inputs) to the facilitation of anxiety-like behaviors. Then positive allosteric modulator of mGluR5 might restore pyramidal neuronal excitability and anxiety-like behaviors.

In summary, we clarified that the expression of mGluR5 in hippocampal CA1 was associated with anxiety-like behavior. In addition, we provide the first evidence that both cellular and behavioral phenotypes of chronic restraint stress could be rescued by CDPPB, confirming a crucial role for mGluR5 signaling in regulating anxiety- like behavior.

REFERENCES

1. Remes O, Brayne C, van der Linde R, Lafortune L. A systematic review of reviews on the prevalence of anxiety disorders in adult populations. Brain Behav. 2016;6:e00497.
2. Huang SH, Liu WZ, Qin X, Guo CY, Xiong QC, Wang Y, et al. Association of increased amygdala activity with stress-induced anxiety but not social avoidance behavior in mice. Neurosci Bull. 2022;38:16–28.
3. Kessler RC, Berglund P, Demler O, Jin R, Merikangas KR, Walters EE. Lifetime preva- lence and age-of-onset distributions of DSM-IV disorders in the National Comorbidity Survey Replication. Arch Gen Psychiatry. 2005;62:593–602.
4. Luo ZY, Huang L, Lin S, Yin YN, Jie W, Hu NY, et al. Erbin in amygdala parval- bumin- positive neurons modulates anxiety-like behaviors. Biol Psychiatry. 2020;87:926–36.
5. Bluett EJ, Homan EJ, Morrison KL, Levin ME, Twohig MP. Acceptance and commit- ment therapy for anxiety and OCD spectrum disorders: an empirical review. J Anxiety Disord. 2014;28:612–24.
6. Ross RA, Foster SL, Ionescu DF. The role of chronic stress in anxious depression. Chronic Stress 2017;1:2470547016689472.
7. Kim KS, Han PL. Optimization of chronic stress paradigms using anxiety- and depre- ssion-like behavioral parameters. J Neurosci Res. 2006;83:497–507.
8. Pal MM. Glutamate: The master neurotransmitter and its implications in chronic tress and mood disorders. Front Hum Neurosci. 2021;15:722323.
9. Acher FC, Cabayé A, Eshak F, Goupil-Lamy A, Pin JP. Metabotropic glutamate receptor orthosteric ligands and their binding sites. Neuropharmacology 2022;204:108886.
10. Bodzęta A, Scheefhals N, MacGillavry HD. Membrane trafficking and positioning of mGluRs at presynaptic and postsynaptic sites of excitatory synapses. Neuro- phar- Macol. 2021;200:8799.
11. McCullock TW, Kammermeier PJ. The evidence for and consequences of meta- botro- pic glutamate receptor heterodimerization. Neuropharmacology 2021;199:108801.
12. Esterlis I, Holmes SE, Sharma P, Krystal JH, DeLorenzo C. Metabotropic Glutamat- ergic Receptor 5 and Stress Disorders: Knowledge Gained From Receptor Imaging Studies. Biol Psychiatry. 2018;84:95–105.
13. Lin S, Li X, Chen YH, Gao F, Chen H, Hu NY, et al. Social isolation during ado- lescence induces anxiety behaviors and enhances firing activity in BLA pyramidal neurons via mGluR5 upregulation. Mol Neurobiol. 2018;55:5310–20.
14. Spooren WP, Vassout A, Neijt HC, Kuhn R, Gasparini F, Roux S, et al. Anxiolytic-like effects of the prototypical metabotropic glutamate receptor 5 antagonist 2- methyl-6- (phenylethynyl) pyridine in rodents. J Pharm Exp Ther. 2000;295:1267–75.
15. Klodzinska A, Tatarczyńska E, Chojnacka-Wójcik E, Nowak G, Cosford NDP, Pilc A. Anxiolytic-like effects of MTEP, a potent and selective mGlu5 receptor agonist does not involve GABA(A) signaling. Neuropharmacology 2004;47:342–50.
16. Fanselow MS, Dong HW. Are the dorsal and ventral hippocampus functionally distinct structures? Neuron 2010;65:7–19.

17. Ross TW, Easton A. The hippocampal horizon: constructing and segmenting experience for episodic memory. Neurosci Biobehav Rev. 2022;132:181–96.
18. Dang R, Zhou Y, Zhang Y, Liu D, Wu M, Liu A, et al. Regulation of Social Memory by Lateral Entorhinal Cortical Projection to Dorsal Hippocampal CA2. Neurosci Bull. 2022;38:318–22.
19. Günther A, Luczak V, Gruteser N, Abel T, Baumann A. HCN4 knockdown in dorsal hippocampus promotes anxiety-like behavior in mice. Genes Brain Behav. 2019;18:e12550.
20. Abela AR, Browne CJ, Sargin D, Prevot TD, Ji XD, Li ZX, et al. Median raphe serotonin neurons promote anxiety-like behavior via inputs to the dorsal hippocampus. Neuropharmacology 2020;168:107985.
21. Chang S, Bok P, Tsai CY, Sun CP, Liu H, Deussing JM, et al. NPTX2 is a key component in the regulation of anxiety. Neuropsychopharmacology 2018;43:1943–53.
22. Parfitt GM, Nguyen R, Bang JY, Aqrabawi AJ, Tran MM, Seo DK, et al. Bidirectional Control of Anxiety-Related Behaviors in Mice: Role of Inputs Arising from the Ventral Hippocampus to the Lateral Septum and Medial Prefrontal Cortex. Neuropsycho- Pharmacol. 2017;42:1715–28.
23. Jimenez JC, Su K, Goldberg AR, Luna VM, Biane JS, Ordek G, et al. Anxiety cells in a hippocampal-hypothalamic circuit. Neuron 2018;97:670–83.
24. Buynitsky T, Mostofsky DI. Restraint stress in biobehavioral research: Recent developments. Neurosci Biobehav Rev. 2009;33:1089–98.
25. Yang Y, Cui YH, Sang KN, Dong YY, Ni ZY, Ma SS, et al. Ketamine blocks bursting in the lateral habenula to rapidly relieve depression. Nature 2018;554:317–22.
26. Mah L, Szabuniewicz C, Fiocco AJ. Can anxiety damage the brain? Curr Opin Psychiatry. 2016;29:56–63.
27. Verpelli C, Dvoretskova E, Vicidomini C, Rossi F, Chiappalone M, Schoen M, et al. Importance of Shank3 protein in regulating metabotropic glutamate receptor 5 (mGluR5) expression and signaling at synapses. J Biol Chem. 2011;286:34839–50.
28. Kubota J, Mikami Y, Kanemaru K, Sekiya H, Okubo Y, Iino M. Whisker experience-dependent mGluR signaling maintains synaptic strength in the mouse adolescent cortex. Eur J Neurosci. 2016;44:2004–14.
29. Bekhbat M, Mukhara D, Dozmorov MG, Stansfield JC, Benusa SD, Hyer MM, et al. Adolescent stress sensitizes the adult neuroimmune transcriptome and leads to sex-specific microglial and behavioral phenotypes. Neuropsychopharmacology 2021;46:949–58.
30. Lei T, Dong D, Song MY, Sun YF, Liu XF, Zhao H. Rislenemdaz treatment in the lateral habenula improves despair-like behavior in mice. Neuropsychopharmacology 2020;45:1717–24.
31. Aubry AV, Khandaker H, Ravenelle R, Grunfeld IS, Bonnefil V, Chan KL, et al. A diet enriched with curcumin promotes resilience to chronic social defeat stress. Neuropsychopharmacology 2019;44:733–42.
32. Fischell J, Dyke AMV, Kvarta MD, LeGates TA, Thompson SM. Rapid Antidepressant Action and Restoration of Excitatory Synaptic Strength After Chronic Stress by Negative Modulators of Alpha5-Containing GABAA Receptors. Neuropsychopharmacology. 2015;40:2499–509.
33. Yim YS, Han W, Seo J, Kim CH, Kim DG. Differential mGluR5 expression in response to the same stress causes individually adapted hippocampal network activity. Biochem Biophys Res Commun. 2018;495:1305–11.
34. Lu YM, Jia Z, Janus C, Henderson JT, Gerlai R, Wojtowicz JM, et al. Mice Lacking Metabotropic Glutamate Receptor 5 Show Impaired Learning and Reduced CA1 Long-Term Potentiation (LTP) But Normal CA3 LTP. J Neurosci. 1997;17:5196–205.
35. Xu J, Zhu YL, Contractor A, Heinemann SF. Metabotropic glutamate receptor 5 (mGluR5) has a critical role in inhibitory learning. J Neurosci. 2009;29:3676–84.
36. Barnes SA, Pinto-Duarte A, Kappe A, Zembrzycki A, Metzler A, Mukamel EA, et al. Disruption of mGluR5 in parvalbumin-positive interneurons induces core features of neurodevelopmental disorders. Mol Psychiatry. 2015;20:1161–72.
37. Xu J, Antion MD, Nomura T, Kraniotis S, Zhu YL, Contractor A. Hippocampal Metaplasticity Is Required for the Formation of Temporal Associative Memories. J Neurosci. 2014;34:16762–73.
38. Kim CS, Chang PY, Johnston D. Enhancement of Dorsal Hippocampal Activity by Knockdown of HCN1 Channels Leads to Anxiolytic- and Antidepressant-like Behaviors. Neuron 2012;75:503–13.
39. Sun XD, Li L, Liu F, Huang ZH, Bean JC, Jiao HF, et al. Lrp4 in astrocytes modulates glutamatergic transmission. Nat Neurosci. 2016;19:1010–8.
40. Pérez MA, Peñaloza-Sancho V, Ahumada J, Fuenzalida M, Dagnino-Subiabre A. n-3 Polyunsaturated fatty acid supplementation restored impaired memory and GABAergic synaptic efficacy in the hippocampus of stressed Rats. Nutr Neurosci. 2018;21:556–69.
41. Mei L, Zhou Y, Sun Y, Liu H, Zhang DW, Liu PP, et al. Acetylcholine muscarinic receptors in ventral hippocampus modulate stress-induced anxiety-like behaviors in mice. Front Mol Neurosci. 2020;13:598811.
42. Hu W, Zhang MY, Czéh B, Flügge G, Zhang WQ. Stress impairs GABAergic network function in the hippocampus by activating nongenomic glucocorticoid receptors and affecting the integrity of the parvalbumin-expressing neuronal network. Neuropsychopharmacology 2010;35:1693–707.
43. Li MX, Li Q, Sun XJ, Luo C, Li Y, Wang YN, et al. Increased Homer1-mGluR5 mediates chronic stress-induced depressive-like behaviors and glutamatergic dysregulation via activation of PERK-eIF2α. Prog Neuropsychopharmacol Biol Psychiatry. 2019;95:109682.
44. Liu CY, Jiang XX, Zhu YH, Wei DN. Metabotropic glutamate receptor 5 antagonist 2-methyl-6-(phenylethynyl)pyridine produces antidepressant effects in rats: Role of brain-derived neurotrophic factor. Neuroscience 2012;223:219–24.
45. Singh B, Henneberger C, Betances D, Arevalo MA, Rodríguez-Tébar A, Meier JC, et al. Altered balance of glutamatergic/GABAergic synaptic input and associated changes in dendrite morphology after BDNF expression in BDNF-deficient hippocampal neurons. J Neurosci. 2006;26:7189–7200.
46. Spyrka J, Hess G. Repeated Neck Restraint Stress Bidirectionally modulates Excitatory Transmission in the Dentate Gyrus and Performance in a Hippocampus-dependent Memory Task. Neuroscience 2018;379:32–44.
47. Charalambakis NE, Govindaiah G, Campbell PW, Guido W. Developmental remodeling of thalamic interneurons requires retinal signaling. J Neurosci. 2019;39:3856–66.
48. Chung G, Shim HG, Kim CY, Ryu HH, Jang DC, Kim SH, et al. Persistent activity of metabotropic glutamate receptor 5 in the periaqueductal gray constrains emergence of chronic neuropathic pain. Curr Biol. 2020;30:4631–42.
49. Chong CH, Li Q, Mak PHS, Ng CCP, Leung EHW, Tan VH, et al. Lrrc7 mutant mice model developmental emotional dysregulation that can be alleviated by mGluR5 allosteric modulation. Transl Psychiatry. 2019;9:244.
50. Yu W, Kwon J, Sohn JW, Lee SH, Kim S, Ho WK. mGluR5-dependent modulation of dendritic excitability in CA1 pyramidal neurons mediated by enhancement of persistent Na^+currents. J Physiol. 2018;596:4141–56.
51. Li DP, Zhu LH, Pachuau J, Lee HA, Pan HL. mGluR5 Upregulation increases excitability of hypothalamic presympathetic neurons through NMDA receptor trafficking in spontaneously hypertensive rats. J Neurosci. 2014;34:4309–17.
52. Chen M, Shu S, Yan HH, Pei L, Wang ZF, Wan Q, et al. Hippocampal Endothelin-1 decreases excitability of pyramidal neurons and produces anxiolytic effects. Neuropharmacology 2017;118:242–50.

AUTHOR CONTRIBUTIONS

T-MG proposed the concept and designed the experiments. XL, Z-JD. J-NX, Z-ML, SL, HC, and S-JL performed the experiments. XL, Z-JD, and X-WL analyzed the results. XL and Z-JD interpreted the results. T-MG, J-MY, and XL wrote and edited the manuscript.

FUNDING

This work was supported by grants from the STI2030-Major Projects (2021ZD0202704), the National Natural Science Foundation of China (82090032, 31830033, 32200950), the Key-Area Research and Development Program of Guangdong Province (2018B030334001, 2018B030340001), the Science and Technology Program of Guangzhou (202007030013), Basic and Applied Basic Research Foundation of Guangdong Province, China (2022A1515011106).

COMPETING INTERESTS

The authors declare no competing interests.

ADDITIONAL INFORMATION

Supplementary information The online version contains supplementary material available at https://doi.org/10.1038/s41386-023-01548-w.

Correspondence and requests for materials should be addressed to Tian-Ming Gao.

Reprints and permission information is available at http://www.nature.com/reprints

Publisher's note Springer Nature remains neutral with regard to jurisdictional claims in published maps and institutional affiliations.